ELSEVIER

Ceramics International 31 (2005) 33–38

CERAMICS INTERNATIONAL

www.elsevier.com/locate/ceramint

Effect of grain size on thermal shock resistance of Al_2O_3–TiC ceramics

X.Q. You [a], T.Z. Si [a], N. Liu [a,*], P.P. Ren [a], Y.D. Xu [a], J.P. Feng [b]

[a] *Department of Materials Science and Engineering, Hefei University of Technology, Hefei 230009, PR China*
[b] *The Center of Mechanics Testing, University of Science and Technology of China, PR China*

Received 24 November 2003; received in revised form 23 December 2003; accepted 22 February 2004
Available online 26 June 2004

Abstract

In this paper, thermal shock resistance of pure hot-pressed alumina and Al_2O_3–TiC composites was studied. In order to assess the influence of Al_2O_3 and TiC starting powder size on thermal shock resistance, Al, Al_2O_3–TiC composites with different particle size were fabricated. The addition of TiC into alumina matrix remarkably improves the mechanical properties and thermal shock resistance. Decreasing grain size can improve the thermal shock resistance, and increase in density improves thermal shock resistance ever further. The critical thermal shock temperature difference (ΔT_c) of Al_2O_3 (powder size 0.24 μm)–TiC (powder size 0.32 μm) composite is 100 °C higher than the ΔT_c of monolith.

Keywords: B. Composites; C. Thermal shock resistance; C. Mechanical properties; D. Al_2O_3; Starting powder size; TiC

1. Introduction

Alumina ceramics, one of extensively utilised structural ceramics, have great potential to be used in many special applications where low density, high hardness, chemical inertness and good high temperature properties are required [1,2]. But alumina is a brittle material with poor fracture toughness and thermal shock resistance. It has been known for many years that the incorporation of a second phase particulate into a ceramic matrix can bring about improvement on the mechanical properties of ceramics. The addition of a secondary phase into a ceramic matrix has been indicated to improve the resistance to crack initiation and propagation in various ways [3–5]. TiC, a common hard alloy powder, was extensively utilised in Al_2O_3–TiC [6] and TiC-based cermets [7] cutting tools owing to their good comprehensive properties such as high hardness, good chemical stability and excellent wear resistance, and improved the thermal shock resistance due to the good physical and chemical match between TiC and Al_2O_3. The addition of TiC into Al_2O_3 matrix has been indicated to improve the flexural strength, fracture toughness and thermal shock resistance, it is attributed to suppression of cracks initiation and propagation by the mechanisms of crack blunting, micro-cracks and cracks deflection accompanied by TiC particle pulling-out.

The classic theory on the thermal shock resistance of brittle ceramics was established by Hasselman [8,9]. In the theory, some thermal shock resistance parameters (R, R^{IV}, etc.) were introduced to evaluate resistance of crack initiation and propagation or strength degradation after a severe thermal shock. It is well-known that rapid temperature changes (thermal shock) can cause serious structural damage to ceramic materials. Thermal shock of ceramics often yields an thermal stress, which is, in some case, sufficient to cause considerable cracking damage or even catastrophic failure. As for Al_2O_3–TiC ceramic tool material, thermal shock-induced crack is one of the main reasons for its fracture when machining at high speed [10].

The aim of the present work was to compare the thermal shock resistance of Al_2O_3–TiC composites with varying particle size with the monolith.

2. Experimental

2.1. Staring materials and sample preparation

The materials used in this study were hot-pressed sintered monolith and Al_2O_3–TiC composites with an incorporation of 30 wt.% TiC. Throughout this paper, A, A1–A3 refers

* Corresponding author.
E-mail address: ningliu@mail.hf.ah.cn (N. Liu).

0272-8842/$30.00
doi:10.1016/j.ceramint.2004.02.009

Table 1
Materials studied and sintering temperature

Material	Al_2O_3		TiC		Sintering temperature (°C)
	Weight percent	Powder size (μm)	Weight percent	Powder size (μm)	
A	100	0.24	0		1650
A1	70	3.12	30	1.36	1750
A2	70	3.12	30	0.32	1700
A3	70	0.24	30	0.32	1650

to the series of alumina ceramics, starting powder size and sintering temperature of are summarised in Table 1.

Powders of Al_2O_3, TiC were ultra-sonically dispersed for 1 h, and mixed thoroughly in proper mass proportions. The mixing was done in a planetary ball mill (QM-1SP) for 2 h by agate balls. A ball to powder mass ratio is 7:1 and the alcohol to powder mass ratio is 2:1. The mixture was dried for 24 h and grinded, then placed in a graphite crucible coated with BN, sintered at 1650–1750 °C, 30 MPa for 1 h in a nitrogen atmosphere. The sintering temperatures for Al_2O_3 and Al_2O_3–TiC ceramics were chosen as the minimum to give near-full density in each case (Table 1).

Rectangular bar specimens of size 30 mm × 4 mm × 3 mm were used for all tests. The bars were ground with a diamond wheel and polished using diamond pastes. The final diamond lap had an abrasive particle of size 0.5 μm before fracture strength testing and the specimen edges were slightly bevelled on a 1200-grit emery paper to remove notches introduced in the course of machining.

2.2. Characterisation techniques

The density and mechanical properties of all sintered materials are given in Table 2. The density of all sintered samples was measured by the Archimedes' method. The volume fraction of porosity (Vf_p) present within the samples was calculated from the relative density.

The hardness (H) and fracture toughness (K_{IC}) at room temperature were evaluated by the Vickers indentation technique. Five indents were made in a row at the middle of each sample to obtain average values. The fracture toughness was calculated by the indentation method according to [11], see Eq. (1):

$$K_{IC} = 0.203 \left(\frac{a}{c}\right)^{-3/2} a^{1/2} H \quad (1)$$

Table 2
Relative density and mechanical properties of materials

Material	Relative density (%)	σ_f (MPa)	H_V (GPa)	K_{IC} (MPa m$^{1/2}$)
A	97	419	17	3.42
A1	99.6	604	21.9	6.12
A2	99.8	695	21.7	6.48
A3	95.2	567	18.9	3.96

The characteristic dimensions of the impressed half-diagonal (a) and the radial/median crack length (c) were measured using an optical microscope.

X-ray diffraction for phase identification of monolith and composites, the results show the phase of monolith is α-Al_2O_3 and the phases of composites are α-Al_2O_3 and TiC. The ground, polished, thermally etched and Au-coated surface microstructure of samples were examined on the XL30-ESEM scanning electron microscope (SEM) at an accelerating voltage of 20 kV. The Au-coated fracture surfaces were examined on LEO-1530VP field emission electron microscope (FEEM).

2.3. Thermal shock experiments

Ground and polished rectangular bars for thermal shock testing were heated to the desired temperatures and held for 30 min in a preheated furnace before quenching by dropping into a bath of water at room temperature. ΔT, the temperature differences for all ceramic materials were chosen referring to literature [10,12,13]. The experiment temperature differences are 150, 200, 240, 250, 260, 300, 400 and 500 °C, respectively. Repetitive thermal shock temperature differences are 100, 150, 200, 250, 300 and 400 °C, respectively, and the number of cycles was five. The flexural strength of the specimens before and after the water quench was measured using a three-point bend test on a Shimadzu DCS-5000 universal testing machine. The loading span was 24 mm, and the cross-head speed was 0.5 mm/min. The mean strength for each of the conditions studied was obtained using six specimens.

3. Results and discussion

3.1. Microstructural features and mechanical properties

Table 2 shows relative density and mechanical properties. The flexural strength (σ_f), fracture toughness (K_{IC}) and hardness (H_V) of all composites is remarkably higher than monolith alumina ceramic. It is well-recognised that the presence of the TiC second phase in the composite can, to some extent, lead to crack deflection and divergence as well as the internal stress induced by the thermal mismatch between TiC and Al_2O_3, can blunt and arrest micro-crack. Fig. 1 shows

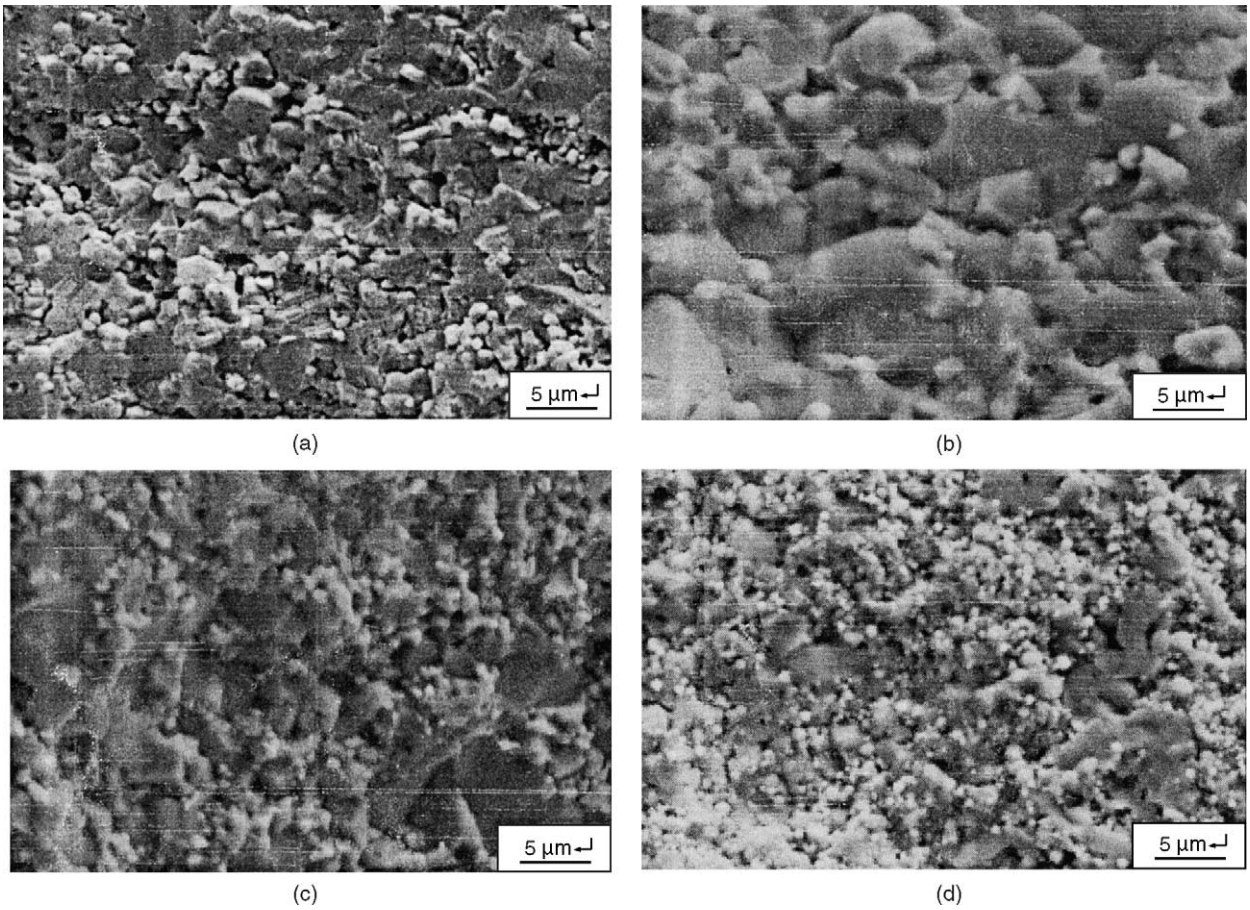

Fig. 1. Fracture surface micrographs of all materials: (a) A, (b) A1, (c) A2, (d) A3.

fractographs of all materials, in that the alumina shows the appearance of the nearly completely intergranular fracture and flat fracture surface, whereas all composites show a degree of transgranular fracture and accompanying TiC particles pulling-out. The addition of TiC particles decreased the Al_2O_3 grain size (see Fig. 2a and d). Therefore, the mechanical properties of composites were improved. Fig. 2 shows typical composite microstructure, white phase is TiC, Gary phase is Al_2O_3. From A1 to A3, the grains were fined by controlling starting powder size of TiC and Al_2O_3, therefore, the mechanical properties of A2 is higher than that of A1. However, fine starting powder introduced difficulty with the densification of A3 (relative density is 95.2%), so its mechanical properties decreased.

3.2. Single thermal shock

According to the Hasselman's theory, the residual strength of material after water quenching is an important index of the thermal shock resistance. Thermal stress fracture resistance parameter R was introduced to estimate thermal stress fracture resistance of materials:

$$\Delta T_{\max} = R = \sigma_f \frac{(1-v)}{E\alpha} \quad (2)$$

where σ_f is the flexural strength, v is the Poisson ratio, E is the Young modulus of elasticity, α is the coefficient of thermal expansion. For severe thermal shocked ceramic materials, critical temperature function R introduce critical thermal stress σ_c, so it is critical temperature difference ΔT_c.

In the current study, specimens of the hot pressed composites and monolith were subjected to a range of temperature differentials by water quenching. The retained flexural strength was then measured in the same way as in Section 2.3. Fig. 3 shows a plot of retained flexural strength versus temperature difference (ΔT) for A, A1–A3. Fig. 3 also show a three-stage behaviour of flexural strength, it is co-incidence with the Hasselman's theory. The curve for the monolith alumina is similar to that reported in the literature [14–16], indicating a critical temperature difference (ΔT_c) of 200 °C and the characteristic sharp loss of flexural strength at the point, followed by a gradual decrease for further increasing. ΔT_c of A1–A3 is 260, 300, 250 °C, respectively. All composites show appreciably greater ΔT_c and residual strength after ΔT_c than monolith. The results demonstrate that the addition of TiC in alumina modifies the composites thermal and mechanical properties and, hence improve the thermal shock behaviours.

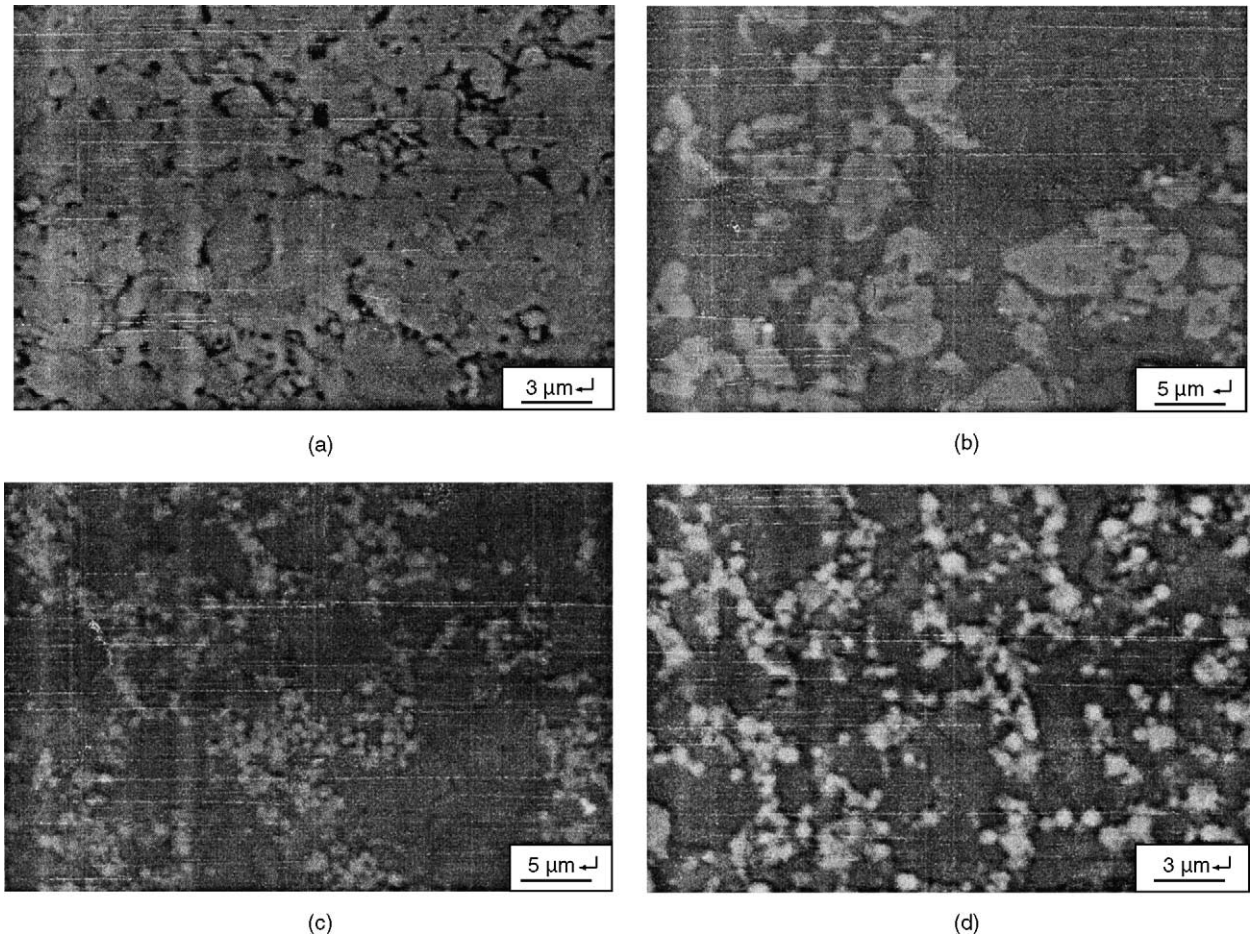

Fig. 2. BSE (back scattering electron) microstructure images of materials studied: (a) A, (b) A1, (c) A2, (d) A3.

In Section 3.1, the mechanical properties of all composites show a remarkable improvement, especially, the higher σ_f and K_{IC} inducted the thermal shock resistance improvement of all composites. The TiC particles suppress crack initiation and propagation, and change the monolith intergranular fracture to composites intergranular and transgranular fracture, which make a contribution to improvement of composite ceramics thermal shock resistance.

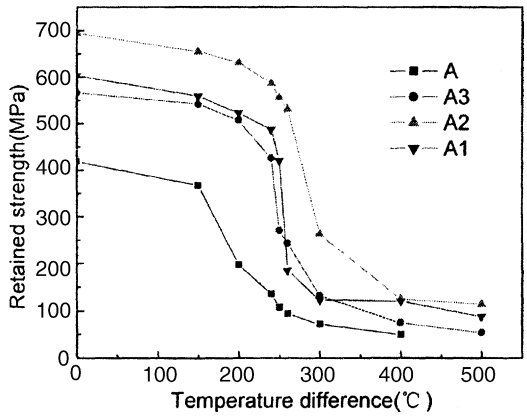

Fig. 3. The retained flexural strength (average) of all materials at various thermal shock temperature difference for single thermal shock.

It is well-known, fined grains can improve mechanical properties of materials. The grains of A2 is finer than that of A1, so mechanical properties of A2 is higher, in which case, the thermal shock resistance is outstanding. The grains of A3 is finer that of A2, but its density is lowest so that its mechanical properties and thermal resistance is the lowest among A1–A3.

One of the most commonly used forms of equation describes the effect of porosity on mechanical properties as [17,18]:

$$X = X_0 \exp(-b\mathrm{Vf_p}) \tag{3}$$

where X is the mechanical property, $\mathrm{Vf_p}$ is the volume fraction of porosity, b is an empirical constant and the subscript 0 indicates zero porosity. From Eq. (3) can conclude Eq. (4):

$$R = \sigma_0 \exp\frac{(-b_\sigma \mathrm{Vf_p})(1-v)}{\alpha E_0 \exp(-b_E \mathrm{Vf_p})} \tag{4}$$

where b_σ, b_E, respectively is empirical constant for the strength and Young modulus of ceramic materials. Usually, $b_E < b_\sigma$ [19–21], so the higher the $\mathrm{Vf_p}$ is, the lower the R is, the thermal shock resistance of materials is poor.

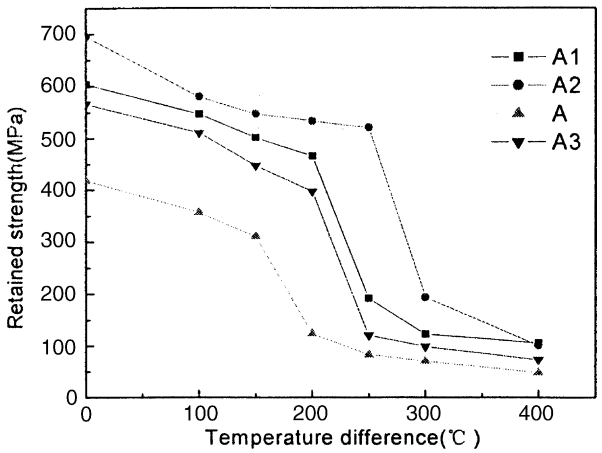

Fig. 4. The retained flexural strength (average) of all materials at various thermal shock temperature difference for repeated thermal shocks.

3.3. Repeated thermal shocks

Ceramic materials inevitable contain some flaws in the form of porosity, micro-cracks, impurity and so on. When containing inherent flaws ceramics are subjected to severe thermal shock, damage at tips of those preexisting flaws will be generated and hence the strength is degraded. The change in strength as a function of the cumulative number of thermal shock cycles is presumably because of the accumulation and coalescence of thermal-shock-induced micro-crack damage. The thermal stress damage resistance parameter R^{IV} was calculated by:

$$R^{IV} = \frac{K_{IC}^2}{\sigma_f^2(1-\upsilon)} \quad (5)$$

Fig. 4 shows a plot of retained flexural strength versus temperature difference on five cycles thermal shock for all materials. It shows the ΔT_c of all four materials is similar to single thermal shock, but the retained flexural strengths are lower for all materials relative to single thermal shock. At $\Delta T = 200\,^{\circ}C$, the retained flexural strength of monolith is 124 MPa, have a remarkable decrease; but that of A1–A3 composites is 466, 534, and 398 MPa, respectively, have a minor decrease. The cumulative of thermal shock cycles inducted thermal stress cumulative damage of materials, but this is clearly shown in Fig. 5, incorporation of TiC particles into alumina matrix can bring about crack deflection, micro-cracks and pinning, etc. which improve the K_{IC} and the thermal shock damage resistance of the composites.

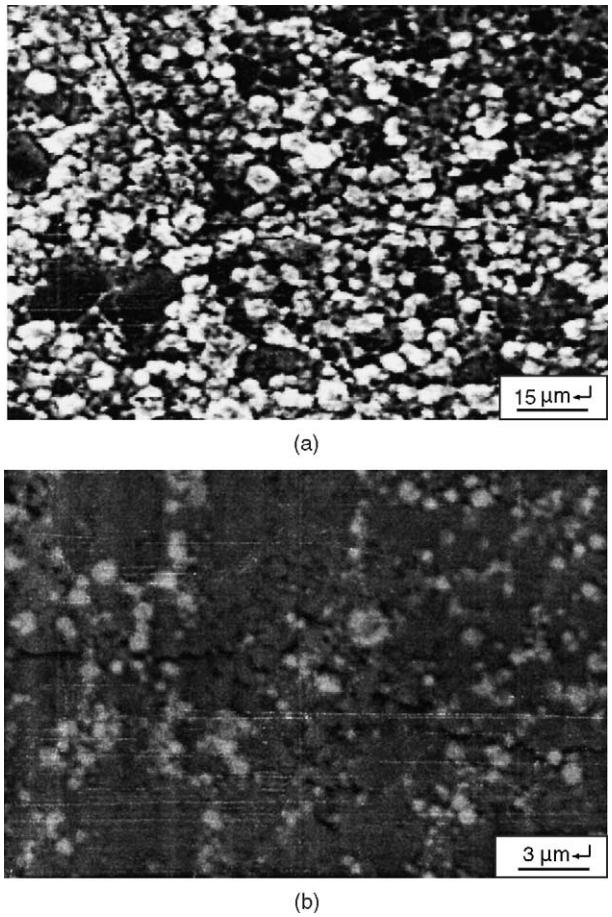

Fig. 5. Photomicrograph showing (a) crack deflection; (b) micro-crack and crack pining of composites.

4. Conclusions

From the results mentioned above, the following conclusions may be shown:

1. The addition of TiC into alumina matrix remarkably improves the mechanical properties and thermal shock resistance.
2. Fined grains also can improve the mechanical properties and thermal shock resistance of composites. But the densification of materials is vitally important to mechanical and thermal shock behaviour. The ΔT_c of A2 composite is 100 °C higher than monolith by controlling the TiC and Al_2O_3 starting powder size.
3. Repeated thermal shocks and single thermal shock of all materials shows similar results, the critical thermal shock temperature difference (ΔT_c) is ranked: A2 > A1 > A3 > A.

References

[1] C.E. Borsa, N.M.R. Jones, R.I. Todd, Influence of processing on the microstructural development and flexural strength of Al_2O_3/SiC nanocomposites, J. Eur. Ceram. Soc. 17 (1997) 865–872.
[2] T. Sekine, T. Nakajima, S. Ueda, K. Nühara, Reduction and sintering of a nickel-dispersed-alumina composite and its properties, J. Am. Ceram. Soc. 80 (1997) 1139–1148.
[3] S. Fayette, D.S. Smith, A. Smith, C. Martin, Influence of grain size on the thermal conductivity of tin oxide ceramics, J. Eur. Ceram. Soc. 20 (2000) 297–302.

[4] M.E. Ebrabimi, J. Chevalier, G. Fantozzi, Slow crack growth behavior of alumina ceramics, J. Mater. Res. 15 (1) (2000) 142–147.
[5] T. Hirata, A. Katsunori, H. Yamamotto, Sintering behavior of Cr_2O_3–Al_2O_3 ceramics, J. Eur. Ceram. Soc. 20 (2000) 195–199.
[6] C.H. Xu, X. Ai, C.Z. Huang, Fabrication and performance of an advanced ceramic tool material, Wear 249 (2000) 503–508.
[7] N. Liu, Y.D. Xu, Z.H. Li, M.H. Chen, F. Xie, Cutting and wear behaviors of TiC based cermets cutter with nano-TiN modification, Trans. Nonferrous Met. Soc. 13 (4) (2003) 869–875.
[8] D.P.H. Hasselman, Strength behavior of polycrystalline alumina subjected to thermal shock, J. Am. Ceram. Soc. 53 (1970) 490–495.
[9] D.P.H. Hasselman, Unified theory of thermal shock fracture initiation, crack propagation in brittle ceramics, J. Am. Ceram. Soc. 52 (1969) 600–604.
[10] J. Zhao, X. Ai, X.P. Huang, Relationship between the thermal shock behavior and the cutting performance of a functionally gradient ceramic tool, J. Mater. Proc. Technol. 129 (2002) 161–166.
[11] E. Mikio, Physical properties and cutting performance of silicon nitride ceramics, Wear 102 (1985) 195–210.
[12] S. Maensiri, S.G. Roberts, Thermal shock of ground and polished alumina and Al_2O_3/SiC nanocomposites, J. Eur. Ceram. Soc. 22 (2002) 2945–2956.
[13] L. Wang, J.L. Shi, Influence of tungsten carbide particles on resistance of alumina matrix ceramics to thermal shock, J. Eur. Ceram. Soc. 21 (2001) 1213–1217.
[14] O. Sbaizero, G. Pezzotti, Influence of molybdenum particles on thermal shock resistance of alumina matrix ceramics, Mater. Sci. Eng. A 343, 273–281.
[15] L. Wang, J.L. Shi, M.T. Lin, H.R. Chen, D.S. Yan, The thermal shock behavior of alumina–copper composites, Mater. Res. Bull. 36 (2001) 925–932.
[16] M. Aldridge, J.A. Yeomans, The thermal shock behavior of ductile particle toughened alumina composites, J. Eur. Ceram. Soc. 19 (1998) 1769–1775.
[17] W. Duckworth, Discussion of Ryshkewitch paper by Winston Duckworth, J. Am. Ceram. Soc. 36 (1953) 68.
[18] E. Ryshkewitch, Compression strength of porous sintered alumina and zirconia, J. Am. Ceram. Soc. 36 (1953) 65–68.
[19] R.W. Rice, Porosity of Ceramics, Marcel Dekker, ISBN: 0-8247-0151-8, 1998.
[20] Y. Chen, Thermal Shock Behavior of Ceramics with Porous and Layered Structures, Ph.D. Thesis, University of Cambridge, 1999.
[21] R.A. Dorey, J.A. Yeomans, P.A. Smith, Effect of pore clustering on the mechanical properties of ceramics, J. Eur. Ceram. Soc. 22 (2002) 403–409.